HIERARCHICAL CLUSTERING OF INDEPENDENT COMPONENTS EXTRACTED FROM fMRI DATA

N. Vanello*, V. Positano**, M. Milanesi*, M.F. Santarelli**, V. Hartwig**, E. Ricciardi[§], P. Pietrini[§], L. Landini[†]

* Department of Electrical Systems and Automation, Fac. of Engineering, Univ. of Pisa, Pisa, Italy
**MRI Laboratory, CNR Institute of Clinical Physiology, Pisa, Italy
[§] Lab. Clinical Biochemistry, Dept. Experimental Pathology, Univ. of Pisa Med. School, Pisa, Italy
[†]Dept. of Information Engineering, University of Pisa, Pisa, Italy

nicvanel@ifc.cnr.it

Abstract: Independent component analysis (ICA) of functional magnetic resonance imaging (fMRI) data can be employed as an exploratory method. The lack in the ICA model of strong a priori assumptions about the activation related signal or about the noise, leads to difficult interpretations of the results by the experimenters. Moreover, the statistical independence, hypothesized in the model, is only approximated by ICA algorithms. Residual dependencies among the extracted components can be investigated in order to reveal some informative structure in the data. In this work we propose a method based on hierarchical clustering algorithm in order to classify the results of ICA applied to fMRI dataset: the clustering algorithm uses a similarity measure based on mutual information between the extracted components. This method could be useful also to overcome the ambiguity related to the model order selection. The method was tested on simulated datasets. Preliminary results on real data are reported and discussed.

Introduction

Functional exploration of the brain by means of Magnetic Resonance Imaging (fMRI) is a rapidly growing technique: fMRI data analysis methods can be classified in confirmatory, or hypothesis-driven methods, and exploratory or data-driven methods. While the former are used in order to test the validity of the experimenters' hypotheses they do not allow to detect unexpected phenomena, i.e. that are not modelled a priori. On the other hand, the latter gives results that are based on general assumption about the signal generation but are often difficult to be interpreted.

Independent Component Analysis (ICA) is one of the most used exploratory methods and it is based on the assumption of statistical independence of the components extracted. This method has proven its capabilities in order to separate physiological component of different origin, detect unexpected phenomena, as activations transiently time locked with the stimulus, or artefacts related signal changes, as those due to movements [1].

One of the main drawbacks of the ICA approaches is that the extracted components are difficult to be classified since the components do not show an order or relationships among them. Furthermore the best number of components to be extracted, i.e. the model order, is not known a priori.

The hypothesis of statistical independence among the estimated ICs in these models is only approximated: the finite number of observations for each measurement does not allow estimating higher order statistics [2] exploited to search for statistical independence so a residual dependency between the extracted components can still be found. This residual dependency can be used to reveal some structure in the dataset, thus to provide further information about the data. A topographic approach has been suggested for ICA [2] where the model was modified to take into account a topographic order between the extracted components: the distance between two elements in the topographic maps is related to the residual dependency.

In this work we propose a classification criterion using a distance measure between the components derived from an estimate of the mutual information. A hierarchical clustering stage is then applied to these distances set in order to classify spatially independent maps of fMRI and identify interesting groups of components. This method could be used both to reveal informative relationships between the ICs and to give information about the model order, i.e. the best number of independent components to be computed. The proposed method was tested on simulated and experimental fMRI datasets.

Materials and Methods

Datasets from fMRI are formed by a time sequences of images or volumes, acquired while the subject is performing some sensory/motor or cognitive task. The experimental paradigm is a block design, with two different alternating conditions. This task is designed to elicit a blood oxygenation level dependent (BOLD)

ISSN: 1727-1983

signal change detected by the MR equipment, usually by means of gradient echo-echo planar sequences (GE-EPI).

Simulated data: a synthetic brain data set is used [4]. Signal increase in response to neural activation is simulated convolving the time course describing the task with a typical hemodynamic response function. We chose the three parameters gamma variate function defined as $\boldsymbol{h(t) = kt^{8.60} e^{-t/0.547}}$ [5], where k is a constant. The simulated task is a block designed alternating 15 seconds ON with 15 seconds OFF conditions. The total time length of each simulated dataset is three minute for a total number of scans equal to 60. The activated regions are created modulating the baseline intensities of a group of voxels, selected using a mask, with the time series previous described. Activated regions are supposed to be limited in a region of connected voxels and they can be obtained using a mask formed by region smoothed with a gaussian kernel, in order to simulate the point spread function due to the vasculature. The gaussian kernel is a bidimensional one with 3 mm full width half maximum (FWHM) parameter. All the simulations we present in this paper were obtained by defining two activated regions of about 2 centimetres of diameter: in the following we denote these activated regions as region of interest (ROI) number 1 and number 2. The signal change in all the simulations we present here is about 2 percent as compared to the baseline level in the center of the activated regions. Different time delays between the activation time courses of the two regions were simulated: 1.25, 2.5 and 5 seconds.

The noise in the images is supposed to be gaussian distributed with zero mean and variance σ. For each delay value, different noise levels were simulated. The simulated noise standard deviation was 0.33%, 0.66%, 1%, and 1.33% of the mean image value at the baseline level. The contrast to noise ratio, defined as $\boldsymbol{CNR = \Delta S/\sigma}$, where $\boldsymbol{\Delta S}$ is the signal change following an activation, equals to, approximately, 6, 3, 2, 1.5: this is the maximum value at the center of the activated regions.

Real data: Brain activity was measured in a 25-years old right-handed male adult. The subject gave informed consent for the test. The scanner used is a 1.5 Tesla, GE Signa Cv/i. An anatomical images was acquired with a 3D GRASS sequence. The functional scans were gradient echo-EPI with TR=3 sec TE=40 msec, FA=90 degrees, bandwidth 62.5 kHz. Twenty axial slices covering the all brain where acquired with slice thickness of 5 mm, 24 cm FOV, and a in plane 64 x 64 spatial resolution, and the number of time frames was 25. The subject head was restrained with foam in order to avoid big head movements. The subject performed a simple finger tapping sequence with his right hand fingers: the task was a simple block design paradigm alternating 15 sec on with 15 seconds off conditions. The total number of scans was 60 for a total run length of three minutes. Images were spatially realigned and a smoothing operation was performed to enhance signal-to-noise ratio. These pre-processing steps were performed using AFNI [6].

Methods: In spatial ICA we can write the observed data as $\boldsymbol{x}(\nu) = [x_1(\nu), x_2(\nu), \ldots, x_n(\nu)]^{\boldsymbol{T}}$, where x_i is the *i*-th image or volume in the sequence and ν is a spatial index for each volume element (voxel). The observed data $\boldsymbol{x}$, can be written as a linear mixing of spatially ICs s_i:

$$\boldsymbol{x}(\nu) = \boldsymbol{A}\boldsymbol{s}(\nu) \qquad (1)$$

where $\boldsymbol{s}(\nu) = [s_1(\nu), s_2(\nu), \ldots, s_n(\nu)]^{\boldsymbol{T}}$. Both s_i and the mixing matrix $\boldsymbol{A}$ are unknown. In this model x_i and s_i are seen as random variables and ν is an index for the observations of each random variable.

The ICA problem consists in finding an unmixing matrix $\boldsymbol{W}$ as an estimate of $\boldsymbol{A^{-1}}$ so that the estimate of the independent components can be written as $\boldsymbol{\tilde{s} = Wx}$ with the hypothesis that the mixing matrix is invertible. Each estimated component $\boldsymbol{\tilde{s}_i}$ can thus be written as a linear combination of the observed variables $\boldsymbol{\tilde{s}_i = w_i^T x}$, with $\boldsymbol{w_i}$ the i-th column of $\boldsymbol{W}$. The original observations can then be written as $\boldsymbol{x = W^{-1}\tilde{s}}$. Each $\boldsymbol{\tilde{s}_i}$ can be seen as a spatial map, individuating a value for every voxel. The *i*-th spatial fixed map is time modulated by the corresponding time course, given by the *i*-th column of $\boldsymbol{W^{-1}}$.

The ICs can be estimated using a method based on the maximization of the nongaussianity of the $\boldsymbol{\tilde{s}_i}$ [6]. A robust approximation of nongaussianity of a random variable y is given by negentropy that is defined as $J(y) = H(y_{gauss}) - H(y)$ where y_{gauss} is a gaussian random variable with the same variance as y, and $\boldsymbol{H}(\cdot)$ is the entropy function. The model (1) assumes that the number of sources, or ICs, equals the number of observed mixtures. This hypothesis does not hold in general and in many applications, as in ICA of fMRI data, the number of underlying sources is supposed to be less than the number of observed variables, i.e the number of acquired images. This assumption may be not satisfied and the number of underlying sources is supposed to be less than the number of observed mixtures. A data reduction operation is performed as a preprocessing step. This preprocessing step is performed along with a whitening operation: the observed variables $\boldsymbol{x}$ are transformed in uncorrelated variables $\boldsymbol{z}$ with unit variance. This operation allows to simplify the successive algorithmic steps since the unmixing matrix becomes orthogonal with n(n-1)/2 degrees of freedom instead of n^2.

A fast fixed point algorithm [8] can be used to find the weights $\boldsymbol{w_i}$ such that negentropy of $\boldsymbol{\tilde{s}_i}$ is maximized. The algorithm employed, at each step updates the weights $\boldsymbol{w_i}$ as follows

$$\boldsymbol{w_i \leftarrow E\{z g(w_i^T z)\} - E\{g'(w_i^T z)\} w} \quad (2)$$

ISSN: 1727-1983

where $g(\cdot)$ is a nonlinear function of the estimated components used to approximate higher order statistics. Different nonlinear functions can be chosen for different application, depending upon the distribution of the sources to be found: in this work we use $g(\cdot) = \tanh(a_1 y)$ with a_1 constant. It can be shown that maximizing the nongaussianity of uncorrelated variables is the same as minimizing the mutual information between them: as described in the introduction, all the algorithms for ICA lead to components that are only approximately statistically independent.

In order to classify the components and explore the residual dependencies among them, a pairwise distance measure is estimated. The distance between two components s_i and s_j is based upon the definition of mutual information as follows:

$$\boldsymbol{D}(s_i, s_j) = \boldsymbol{H}(s_i, s_j) - \boldsymbol{I}(s_i, s_j) \quad (3)$$

where $\boldsymbol{H}(s_i, s_j)$ is the joint entropy and $\boldsymbol{I}(s_i, s_j)$ is the mutual information between two sources. The choice to use $\boldsymbol{D}(s_i, s_j)$ rather than $\boldsymbol{I}(s_i, s_j)$ is based on the fact that the latter is not a distance in the mathematical sense.

To compute the measure in equation 3, a histogram based technique was used: the estimated sources values are partitioned in bins or intervals. The probability that a variable value, i.e. independent component, lies in the *k*-th interval $\boldsymbol{a_k}$ can be found as the frequency of occurrence, so that we can write $\boldsymbol{p}(\boldsymbol{s_i} \subset \boldsymbol{a_k}) = \frac{\boldsymbol{N_k}}{\boldsymbol{N}}$ where N is the total number of observations for s_i and N_k is the number of times s_i belongs to the *k*-th interval. We'll write this probability as $\boldsymbol{p}(\boldsymbol{a_k})$.

The probability that the variable s_i lies in the *h*-th interval while the variable s_j lies in the *k*-th interval is given by $\boldsymbol{p}(\boldsymbol{s_i} \subset \boldsymbol{a_h}, \boldsymbol{s_j} \subset \boldsymbol{a_k}) = \frac{\boldsymbol{N_{hk}}}{\boldsymbol{N}}$ where N_{hk} is the number of times the couple (s_i, s_j) belongs to the bidimensional bin *[h,k]*. This quantity can be written as $\boldsymbol{p}(\boldsymbol{a_h}, \boldsymbol{a_k})$.

The joint entropy was computed as

$$\boldsymbol{H}(s_i, s_j) = -\sum_{\boldsymbol{h}=1}^{\boldsymbol{N_h}} \sum_{\boldsymbol{k}=1}^{\boldsymbol{N_k}} \boldsymbol{p}(\boldsymbol{a_h}, \boldsymbol{b_k}) log(\boldsymbol{p}(\boldsymbol{a_h}, \boldsymbol{b_k})) \quad (4)$$

while the Mutual Information was computed as

$$\boldsymbol{I}(s_i, s_j) = \sum_{\boldsymbol{h}=1}^{\boldsymbol{N_h}} \sum_{\boldsymbol{k}=1}^{\boldsymbol{N_k}} \boldsymbol{p}(\boldsymbol{a_h}, \boldsymbol{b_k}) log\left(\frac{\boldsymbol{p}(\boldsymbol{a_h}, \boldsymbol{b_k})}{\boldsymbol{p}(\boldsymbol{a_h})\boldsymbol{p}(\boldsymbol{b_k})}\right) \quad (5)$$

where N_h and N_k are the number of states, or bins, for variable s_i and s_j respectively.

An adaptive partitioning operation was applied in order not to have the results blurred by individual distributions of the components [8]. This was obtained by a rank ordering operation of the elements of each independent component.

A hierarchical clustering approach based on the Ward method [10] is proposed to classify and visualize the similarities between the extracted ICs: this method consists in merging every possible cluster pair and choosing the one which minimizes the information loss. A dendrogram can be used to visualize the merging of the components.

In order to correctly interpret the results of the hierarchical clustering algorithm applied to the extracted independent components from simulated datasets, each IC has to be classified. The interesting ICs among the extracted, can be detected looking at the correlation coefficient between the corresponding time courses and the activated region time courses: an independent component whose corresponding time course highly correlates with the activation time course is said to be consistently task-related (CTR) component as in [1]. The spatial accuracy of the independent maps has been evaluated as well as the ability to separate the two activated regions. Each independent map is transformed into a z map statistics as suggested in [1] to find the voxels, in the individual maps, contributing significantly to the respective component: given an independent map s_i the z map can be computed as $\boldsymbol{z} = \frac{\boldsymbol{s_i} - \boldsymbol{m_i}}{\sigma_{\boldsymbol{i}}}$ where m_i is the mean of the values of s_i and σ_i their standard deviation. The performance of the ICA in detecting and separating the activation regions was evaluated using receivers operating characteristics (ROC) curves [11] that are plots of true positive fraction against false positive fraction obtained varying the threshold level of the z maps. The area under curve (AUC)[12] was estimated to assess the detection accuracy of the method: an AUC ranging from 0.7 to 0.8 is considered a results showing a fair accuracy of the test performed, between 0.6 and 0.7 is considered a poor accuracy index. An independent component whose AUC is significant for both ROIs is a component that merges both the two activated regions.

Another ambiguity is given by the effects of model order misspecifications: in fact underestimating the model order may cause an information loss while overestimating the model order may cause overlearning and generate spurious components. For these reasons the method was tested on simulated datasets against different model orders, i.e. number of extracted components: the number of ICs extracted was, for each dataset, equal to 10, 15 and 20.

The same approach was used for the application on real dataset example. In this case it is not possible to estimate an AUC performance parameter, since we don't know a priori the spatial distribution of the activated regions. It is possible to detect interesting components by looking at the correlation coefficient between the associated time course for each map and the expected hemodynamic time course, given the experimental paradigm.

ISSN: 1727-1983

Results

Simulated datasets results: Results from ICA in simulated datasets are summarized in tables 1 2 and 3. The tables refer to results for the delays between the activations time courses equal to 1.25, 2.5 and 5 seconds respectively. The two activated regions are indicated by ROI number 1 and number 2. For each table different noise level results are summarized. The number of the IC whose time course highly correlate with the activation time course of the relevant ROI is indicates in brackets. Since in ICA the extraction order of the independent component cannot be determined, the IC number is important to determine whether a component pertains to a single ROI or both.

Table 1: Evaluation of ICA of the dataset with activations in ROI #1 and ROI #2 with time delay of 1.25 seconds, at different noise levels and model orders. The AUC is shown near the IC number (in brackets).

Activations Delay 1.25 sec	Number of ICs	ROI #1 (IC number) AUC	ROI #2 (IC number) AUC
noise σ=0.33%	10	(3) 0.77 (6) 0.71	(5) 0.77 (4) 0.72
	15	(4) 0.77 (14) 0.77	(1) 0.79 (3) 0.77
	20	(4) 0.76 (13) 0.78	(5) 0.74 (6) 0.69 (9) 0.77
noise σ=0.66%	10	(4) 0.72 (7) 0.72 (8) 0.7	(4) 0.68 (6) 0.72 (7) 0.72
	15	(2) 0.7 (8) 0.75	(4) 0.75 (7) 0.68
	20	(1) 0.71 (11) 0.75 (20) 0.66	(10) 0.73 (11) 0.71 (20) 0.7
noise σ=1.00%	10	(3) 0.7 (7) 0.68 (8) 0.62 (9) 0.67	(3) 0.7 (7) 0.7 (8) 0.7 (9) 0.65
	15	(5) 0.77 (6) 0.77 (12) 0.74 (13) 0.68	(5) 0.75 (6) 0.75 (12) 0.75 (13)0.73
	20	(18) 0.7 (20) 0.73	(18) 0.73 (20)0.74
noise σ=1.33%	10	(2) 0.73 (3) 0.74	(2) 0.7 (3) 0.76
	15	(8) 0.75 (11) 0.67	(8) 0.71 (11) 0.72
	20	(4) 0.72 (20) 0.66	(4) 0.7 (20) 0.73

Table 2: Evaluation of ICA of the dataset with activations in ROI #1 and ROI #2 with time delay of 2.5 seconds, at different noise levels and model orders. The AUC curve is shown near the IC number (in brackets).

Activations Delay 2.5 sec	Number of ICs	ROI #1 (IC number) AUC	ROI #2 (IC number) AUC
noise σ=0.33%	10	(3) 0.78 (8) 0.8	(1) 0.76 (2) 0.74 (9) 0.77
	15	(5) 0.8 (7) 0.8	(9) 0.8 (10) 0.8 (11) 0.71
	20	(2) 0.7 (5) 0.7 (6) 0.7 (15) 0.74	(11) 0.77 (17) 0.79 (19) 0.77
noise σ=0.66%	10	(3) 0.8 (15) 0.78	(5) 0.84 (15) 0.76
	15	(2) 0.77 (8) 0.78	(10) 0.78 (9) 0.8
	20	(5) 0.79 (6) 0.76	(1) 0.78 (2) 0.77
noise σ=1.00%	10	(1) 0.75 (5) 0.8 (7) 0.69	(4) 0.75 (10) 0.76
	15	(1) 0.73 (3) 0.7	(6) 0.7 (14) 0.74 (15) 0.72
	20	(2) 0.68 (6) 0.74	(2) 0.7 (17) 0.79
noise σ=1.33%	10	(4) 0.65 (10) 0. 71	(4) 0.76 (10) 0.61
	15	(11) 0.74 (14)0.65	(11) 0.65 (14) 0.74
	20	(4) 0.74 (16) 0.64	(6) 0.69 (16) 0.67

Table 3: Evaluation of ICA of the dataset with activations in ROI #1 and ROI #2 with time delay of 5 seconds, at different noise levels and model orders. The AUC curve is shown near the IC number (in brackets).

Activations Delay 5 sec	Number of ICs	ROI #1 (IC number) AUC	ROI #2 (IC number) AUC
noise σ=0.33%	10	(3) 0.77 (7) 0.76 (8) 0.78	(5) 0.76 (9) 0.79 (10) 0.76
	15	(6) 0.79 (10) 0.74 (14) 0.78	(4) 0.74 (11) 0.8
	20	(19) 0.9	(8) 0.74 (11) 0.76 (17)0.77
noise σ=0.66%	10	(2) 0.72 (3) 0.77	(5) 0.84
	15	(7) 0.74 (12) 0.76	(2) 0.75 (4) 0.74
	20	(2) 0.76 (3) 0.75	(11) 0.78 (16) 0.75
noise σ=1.00%	10	(9) 0.74 (10) 0.77	(3) 0.76 (7) 0.76
	15	(5) 0.7 (10) 0.68 (15) 0.73	(1) 0.76 (8) 0.73 (11) 0.7
	20	(15) 0.8	(7) 0.76 (13) 0.76
noise σ=1.33%	10	(9) 0.82	(4) 0.76 (5) 0.76
	15	(14) 0.83	(5) 0.71 (11) 0.76
	20	(12) 0.85	(2) 0.76 (15) 0.76

The area under curve (AUC) is indicated as well. In the case of a shorter time delay between the activations time courses of the two ROIs with noise standard deviation greater than 0.33%, the two ROIs cannot be distinguished by the ICA model: so the same IC number appears in both columns. The same results are obtained for a time delay of 2.5 seconds at higher noise levels.

In Figures 1-2 typical dendrograms obtained from clustering operation in simulated datasets are shown.

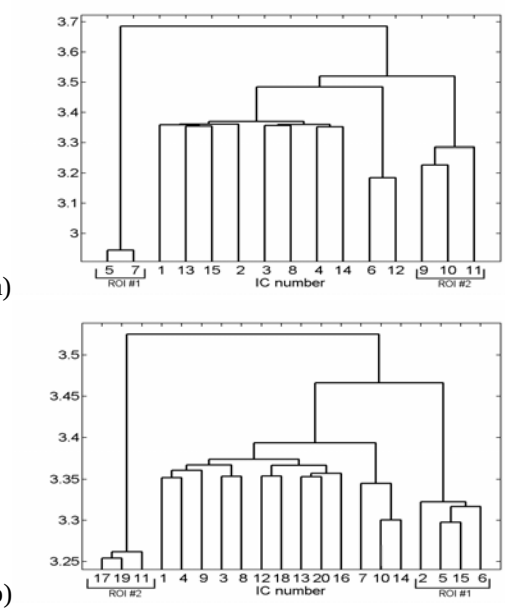

Figure 1: Dendrogram obtained from clustering of the pairwise mutual distances between extracted ICs from simulated datasets in the case of noise level σ=0.33% and time delay 2.5 seconds with model order equal 15 (a) and 20 (b).

In each case the components corresponding to the same activation regions are merged together. In figure 1 the

ISSN: 1727-1983

results for noise level equal to 0.33% and time delay 2.5 seconds are shown. In this case the two regions of activation are distinguished by the ICA model, as can be seen from table 2, and the corresponding ICs are grouped together for each model order. In figure 2 the results for noise level equal to 1% and time delay 1.25 seconds are shown: as it can be seen from table 1, the two activation regions are not distinguished by the ICA model. In both dendrograms the interesting IC components are merged together.

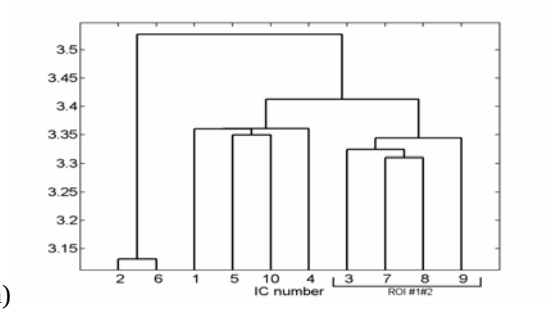

a)

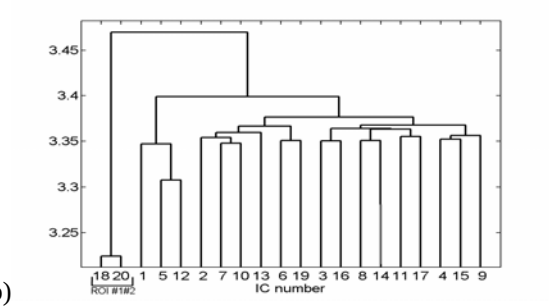

b)

Figure 2: Dendrogram obtained from clustering of the pairwise mutual distances between extracted ICs in the case of noise level σ=1% and time delay 1.25 seconds with model order equal 10 (a) and 20 (b).

Real dataset results: The ICA model applied to real dataset with a model order equal to 10, detected one CTR IC: in figure 3 the corresponding map thresholded for $|z| > 2$ is shown superimposed to an anatomical T1 weighted mask.

The ipsilateral and controlateral primary motor areas are shown along with the supplementary motor area (SMA). Both with model order equal to 20 and equal to 30, two ICs were found to correlate with the experimental paradigm: the results are shown in figures 4 and 5 respectively. The primary motor areas and the SMA were detected by different ICs in both cases. The hierarchical clustering algorithm, as shown in figure 6, succeeded in merging together these components both for model order 20 (figure 6 a) and model order 30 (figure 6 b): the interesting components were merged with some other components that were not identified at a first level, then merged together at a second level.

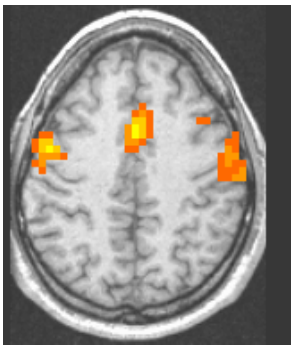

Figure 3: consistently task related (CTR) IC for real dataset with model order equal to 10. The IC map is superimposed upon an anatomical image and thresholded with $|z| > 2$.

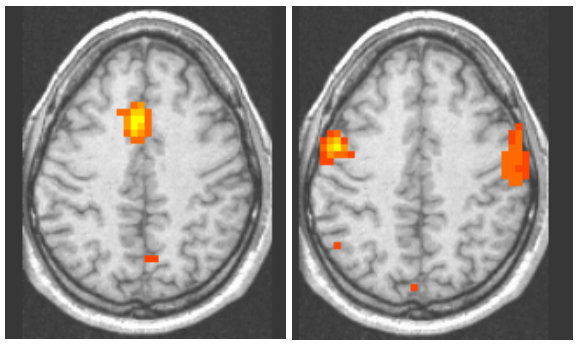

Figure 4: CTR ICs for real dataset with model order equal to 20. On the left the component number 8 is shown pertaining the SMA activity while on the right the component number 7 is shown, pertaining activity in the ipsilateral and controlateral primary motor areas.

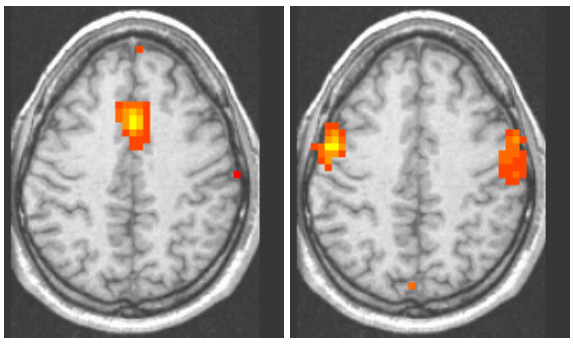

Figure 5: CTR ICs for real dataset with model order equal to 30. On the left the component number 18 is shown pertaining the SMA activity while on the right the component number 15, pertaining activity in the ipsilateral and controlateral primary motor areas, is shown.

ISSN: 1727-1983

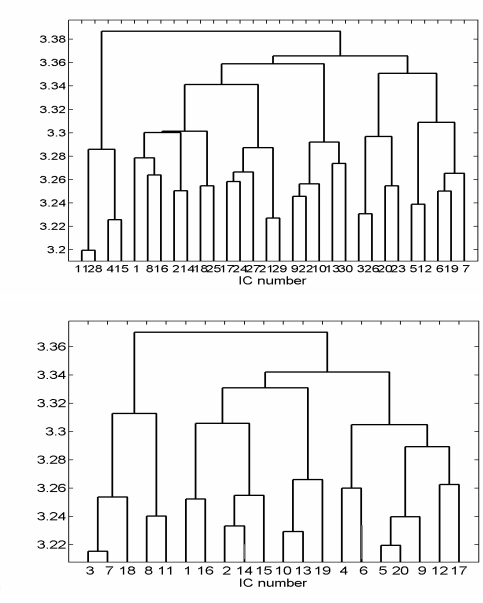

Figure 6: dendrogram obtained from clustering of the pairwise mutual distances between extracted ICs from real data. Figure a refers to 20 ICs model order, while figure b refers to 30 ICs model order.

Discussion

The method proposed aims to study the residual dependencies between the ICs in order to reveal some informative structure in the data as well as face the ambiguities inherent the model order indeterminacy. A similar approach was developed in [13] and used within an ICA framework: the differences regard the choice of the distance measure, the algorithm employed to estimate the independent components, that exploits the minimization of the mutual information [14] and the application field. In this work we have applied the fastICA algorithm used efficiently for analysis of fMRI data [15]. The proximity measure used for clustering, given by equation 3, was estimated using a rank ordering operation: this operation allows to facilitate the computation of mutual information transforming the distributions of the components in uniform distributions. Moreover, since we are interested in similarities between two distributions, this approach allows the results not to be blurred by the individual distributions of the components: in fact, the correlations between two components are preserved, as the validity of the results.

The evaluation of the ICA results has been necessary in order to interpret the results of the hierarchical clustering approach. The interesting ICs were found by looking at the correlation coefficient of the corresponding time course and the modulating time course of each activation region: this value was not given because it was not our purpose to focus on ICA performances. The area under the ROC curve was evaluated to classify the ICs in order to determine the ROI they are related to: as we have seen some components are related to both ROIs, as in the case of time delay equal to 1.25 seconds with mild/high noise levels (see table 1). This is may be due to limitations of ICA algorithm in this case: however as is possible to see from dendrogram analysis, the clustering operation associate, successfully, these components to the same cluster.

The fact that the same region of activation can be separated in different components may be due to problems arising from model order inaccuracy. In this case the clustering approach proposed can be used to overcome this ambiguity: in fact, on the simulated datasets, the clustering algorithm succeeded in grouping together components belonging to the same region of activation found by ICA.

The low values of the AUC parameter may be due to the fact that the same activated region is often decomposed in different ICs: combining the components merged by the clustering algorithm may be a way to reconstruct correctly the activated regions and improve accuracy performances.

These results may be used as a guideline for real data application even if further modelling and analysis are required: the real data example proposed here has been analyzed with larger model orders than those used in simulations since lower orders failed in revealing the correct activated regions. Simulations on null data, as echo planar images acquired in resting conditions, with superimposed simulated activations, may be also used.

The clustering algorithm proved to be able to find similarities between CTR IC maps, independently from the model order used: some components were found to merge with the CTR ones, but it was not possible to identify their origin. Further analysis on real datasets is needed in order to ascertain the validity of the proposed method in fMRI exploratory approaches. One unresolved issue is the choice of a hierarchy level that may distinguish interesting and homogeneous groups from each other.

Conclusions

A hierarchical clustering algorithm has been proposed in order to classify the spatially independent components obtained by ICA. The hypothesis of statistical independence of the extracted components is only approximated by the resulting ICs: the residual dependencies among the components may reveal some informative structure in the data. The clustering algorithm merges the components depending upon a similarity measure derived from the pairwise mutual information among the ICs. This operation has demonstrated successful in simulated dataset in merging together IC maps related to the same activated region found by ICA. Preliminary results on real data seem to indicate that the method merges together ICs belonging to the same phenomenon and encourage further analyses.

ISSN: 1727-1983

Acknowledgments

This work was supported by IST-2002-6.1.1 FET Presence.

References

[1] MCKEOWN, M. J.,MAKEIG, S., BROWN, G., JUNG, T.-P., KINDERMANN, S. S., BELL, A. J., SEJMOWSKI, A. J. (1998): 'Analysis of fMRI data by blind separation into independent spatial components', *Hum. Brain Mapp.*, **6**, pp. 60-188

[2] NIKIAS, C., MENDEL, J. (1993): 'Signal processing with higher-order spectra'. *IEEE Sig. Proc. Mag.*, pp. 10-37

[3] HYVÄRINEN, A., HOYER, P.O., INKI, M. (2001): 'Topographic independent component Analysis'. *Neural Comput.*, **113**, pp. 1527-1558

[4] COCOSCO, C.A., KOLLOKIAN, V., KWAN, R.K.-S., EVANS, A.C. (1997): 'BrainWeb: Online Interface to a 3D MRI Simulated Brain Database'. *NeuroImage*, **5(4)**, S425

[5] COHEN, M.S. (1997): 'Parametric Analysis of fMRI Data Using Linear Systems Methods', *NeuroImage*, **6**, pp. 93-103

[6] COX, R.W. (1996): 'AFNI: software for analysis and visualization of functional magnetic resonance neuroimages'. *Comput. Biomed. Res.*, **29**, pp. 162-173

[7] DELFOSSE, N., LOUBATON, P. (1995): 'Adaptive blind separation of independent sources: a deflation approach'. *Signal Process.*, **45**, pp. 59-83

[8] HYVÄRINEN, A., OJA., E. (1997): 'A fast fixed-point algorithm for independent component analysis', *Neural Comput.*, **9**, pp. 1483-1492

[9] STEUER, R., KURTHS, J., DAUB, C.O., WEISE, J., SELBIG, J. (2002): 'The mutual information: detecting and evaluating dependencies between variables', *Bioinformatics*, **18**(2), S231-S240

[10] WARD, J.H. JR. (1963): 'Hierarchical grouping to optimize an objective function'. *J. Am. Stat. Assoc.* **58**, pp. 236–244

[11] SKUDLARSKI, P., CONSTABLE, R.T., GORE, J.C. (1999): 'ROC Analysis of Statistical Methods Used in functional MRI: Individual subjects', *NeuroImage*, **9**, pp. 311-329

[12] BAMBER, D.C. (1975): 'The area above the ordinal dominance graph and the area below the receiver operating characteristic graph', *J. Math. Psychol.*, **12**, pp.387–415.

[13] KRASKOV, A., STÖGBAUER, ANDRZEJAK, R. G., GRASSBERG, P. (2005): 'Hierarchical clustering using mutual information', *Europhys. Lett.*, **70**(2), pp. 278-284

[14] KRASKOV, A., STÖGBAUER, H., GRASSBERGER, P. (2004): 'Estimating mutual information', *Phys. Rev. E*, **69**(6), 066138

[15] ESPOSITO, F., FORMISANO; E., SEIFRITZ, E., GOEBEL, R, MORRONE, R., TEDESCHI, G., DI SALLE, F. (2002): 'Spatial independent component analysis of functional MRI Time-series: to what extent do results depend on the algorithm used?' *Hum. Brain Mapp.*, **16**, pp. 146-157

ISSN: 1727-1983